RESPIRATORY MOTION COMPENSATION FOR IMAGE-GUIDED BRONCHOSCOPY USING A GENERAL MOTION MODEL

Tobias Klinder, Cristian Lorenz

Philips Research Europe - Hamburg

ABSTRACT

In this paper, we investigate the use of a general motion model for motion compensation of CT/X-ray fusion during image-guided bronchoscopy, where respiratory motion causes a misalignment between the pre-operative CT and the intra-operative X-ray images. The general motion model is learned from four-dimensional images of different patients and captures statistics of lung motion. For motion compensation, the general model can then be individualized using the pre-operative CT, while a surrogate to drive the model can be derived from the X-ray images. Quantitative evaluation was carried out on 4D-CT data. Virtual projections were generated from the 4D-CT data to simulate the intra-operative X-ray images of different breathing states. The average prediction error between maximal inhale and maximal exhale was found to be 4.06 $\pm$ 1.64 mm, which means that the model compensated for 56% of the motion amplitude.

Index Terms— Motion modeling, bronchoscopy, 4D-CT

1. INTRODUCTION

Breathing-induced organ motion impedes many image-guided interventions working on the chest or upper abdomen. One possibility to reduce the uncertainties of breathing motion is by means of a respiratory motion model and various approaches have been presented recently.

Patient-specific models derived from pre-operative four-dimensional data have been proposed, as, e.g., in [1], to adapt to inter-cycle variations. While four-dimensional imaging provides valuable information of patient-specific organ motion, acquisition of four-dimensional data is typically not done for most image-guided interventions due to an increase in treatment costs, change in workflow, and, in the case of 4D-CT, dose issues. In order to overcome these limitations, general motion models have been presented that are learned from four-dimensional data from different subjects [2, 3].

In this paper, we investigate the use of a general motion model for motion compensation of CT/X-ray fusion during image-guided bronchoscopy. In contrast to other applications, where, e.g., breath-holding can be considered, bronchoscopy is usually performed while the patient is under free breathing. When it comes to peripheral lesions, where navigation to the target can not be purely based on a bronchoscope, X-ray guidance is commonly used once the airways are too small. While X-ray images clearly show the bronchoscope and the biopsy device, the drawbacks of fluoroscopy are that soft tissue structures, e.g., the airways or the lesion itself, cannot be seen and only projections are captured. Image-fusion with pre-acquired 3D-CT has been proposed to provide three-dimensional anatomic information during the procedure. However, respiratory motion causes still a mismatch between the pre-operative CT and the intra-operative X-ray.

The main contribution of this paper is the integration of a general statistical motion model in a clinical workflow of a dedicated application. Motion compensation is thereby performed by deriving a surrogate signal directly from the available projection images.

2. METHODS

2.1. System Overview

The overview of the entire set-up for motion compensation is shown in Fig. 1. Motion fields are extracted during learning from four-dimensional data of different subjects and combined in a generalized model. During the application, the pre-operative diagnostic 3D-CT is used to individualize the model. The surrogate to drive the motion model can be extracted by comparing the intra-operative X-ray with a virtual projection image, i.e., a digitally reconstructed radiograph (DRR) generated from the CT image. As latest X-ray systems are able to provide high resolution images covering the complete upper thorax, we use the change of diaphragm position as a surrogate. To generate DRR images from the same perspective as the X-ray image, the pre-operative CT and the X-ray system are registered. Finally, the output of the model is a continuous three-dimensional deformation field, which can be used to warp the volume and computed segmentations according to the X-ray image.

Compared to other often used global surrogates, as, e.g., total lung volume, the change in diaphragm position can be extracted for both lungs individually for many projection angles. Furthermore, the X-ray images allow to extract the internal organ motion, which might give a better correlation as external surrogates, as e.g., tracking of skin markers.

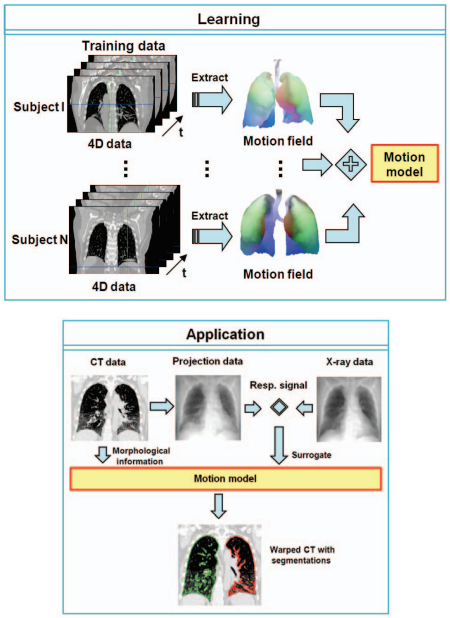


Fig. 1. Set-up for motion compensation. A motion model is learned from motion fields of different subjects. Based on a surrogate signal and the pre-operative CT image, the motion model finally predicts a three-dimensional deformation field.

2.2. Statistical Motion Model

2.2.1. Training Set.

The training set covers free-breathing 4D-CT thorax data sets of 31 patients that were acquired for radiotherapy treatment. Each ten phase 4D-CT represents one respiratory cycle with images $I_0, I_1, \dots I_9$, where I_0 is maximum inhale and I_5 maximum exhale. All images had an in-plane resolution of 0.85-0.97 mm and a slice thickness of 2.5 mm.

2.2.2. Motion Field Extraction.

Lung motion fields are derived from the 4D-CT images using the technique proposed in [4], which has been intensively validated, e.g., in [5]. The output of the motion field estimation are for each patient $p \in \{1, \dots N_p\}$ continuous motion fields $\phi_{j,p}$ between a selected reference phase, which was chosen to be $p = 5$ (maximum exhale), and a phase $j \in \{0, 1, \dots, 4, 6, \dots, 9\}$.

2.2.3. Inter-Subject Registration.

To build a statistical model of respiratory motion, correspondences between different subjects have to be established. As the computed transformations $\phi_{j,p}$ are given with respect to the reference image of patient p, inter-patient correspondences need to be defined between the selected reference images of the N_p patients. However, establishing a dense anatomical correspondence of the lungs between patients is difficult as inside structures like the airways or the vessel tree show varying topologies across patients. Therefore, we estimate the inter-patient transformation $\Phi_{p,q}$ from subject p to q on the basis of the outer surface of the lungs. In each selected reference image of each patient, a shape model covering the outer lung surfaces [6] is adapted. By preserving the mesh topology and restricting the mesh during adaptation to be most similar to the initial model, vertex correspondences provide sparse anatomical correspondences. Based on the adapted surface, a thin-plate spline interpolation provides the dense transformations $\Phi_{p,q}$.

2.2.4. Model Representation.

In order to compare the subject-specific motion fields, we map the transformations $\phi_{j,p}$ into a common space given by the adapted outer surface lung model. Let Ω_M and Ω_p denote the model and the patient space, respectively, and $\Phi_{M,p}$ the transformation from the model to the patient space and $\Phi_{p,M}$ the transformation back to the model space. Then, given a point $\mathbf{x} \in \Omega_M$ with corresponding point $\mathbf{x}' = \Phi_{M,p}(\mathbf{x}) \in \Omega_p$, the point $\mathbf{y}' = \phi_{j,p}(\mathbf{x}')$ transformed by the motion field in Ω_p can be expressed in the model coordinate system as $\mathbf{y} = \Phi_{p,M}(\mathbf{y}')$ which yields the total transformation

$$\tilde{\phi}_{j,p} = \Phi_{p,M} \circ \phi_{j,p} \circ \Phi_{M,p} \tag{1}$$

where $\tilde{\phi}_{j,p}$ gives the subject-specific motion field in the common model space and $\circ$ the composition operation.

For statistical modeling, we consider the motion on a regular grid inside the lung model sampled by 5 mm isotropically and a reduced set of vertices on the outer surface. In total, we take around 1000 locations per lung. Compared to a whole volume, this subset significantly reduces the high computational effort for statistical modeling. In order to re-estimate the continuous transformation, thin-plate spline interpolation based on the subset is again chosen. The displacement of a set of K locations in model space is expressed by the vector $\mathbf{m} = [\delta x_1, \delta y_1, \delta z_1, \dots \delta x_K, \delta y_K, \delta z_K]^T$, where δx_k, δy_k, δz_k gives the displacement in $\mathbf{x}$-, $\mathbf{y}$-, and $\mathbf{z}$-direction of the k-th vertex location. The vector $\mathbf{z}$ is then the concatenation of all phase vectors

$$\mathbf{z} = [\mathbf{m}_0, \mathbf{m}_1, \dots, \mathbf{m}_4, \mathbf{m}_6, \dots, \mathbf{m}_9]^T . \tag{2}$$

The proposed representation is based on the displacement vectors and can be considered as a deformation model, which gives the deformation of a set of landmarks over the breathing cycle. The set of N_p corresponding vectors $\mathbf{z}_n$ is then combined in the matrix $\mathbf{Z} = [\mathbf{z}_1 | \mathbf{z}_2 | \dots | \mathbf{z}_{N_p}]$ and principal component analysis (PCA) is applied

$$\mathbf{z} = \bar{\mathbf{z}} + \mathbf{U}\mathbf{b} , \tag{3}$$

where $\bar{\mathbf{z}}$ is the mean, $\mathbf{U}$ is the matrix containing the eigenvectors and $\mathbf{b}$ is the weight vector.

2.2.5. *Motion Prediction.*

The PCA-model can be used to predict the motion field given a surrogate signal. For that purpose, the vector $\mathbf{z}$ will be partioned into two parts $\mathbf{z} = [\frac{\mathbf{y}}{\mathbf{x}}]$, where $\mathbf{y}$ gives the part to be predicted and $\mathbf{x}$ belongs to the surrogate signal. Equivalent partitions for mean and covariance yield

$$\bar{\mathbf{z}} = \begin{pmatrix} \bar{\mathbf{z}}_y \\ \bar{\mathbf{z}}_x \end{pmatrix} \qquad \mathbf{U} = \begin{pmatrix} \mathbf{U}_y \\ \mathbf{U}_x \end{pmatrix} . \tag{4}$$

To express the statistical model in patient space, it is transformed using the transformation $\Phi_{M,p}$. After transforming the model, motion prediction is carried out by estimating the weight vector $\mathbf{b}$ in Eq. 3 in the subspace spanned by the surrogate signal. The weight vector which gives the solution with minimal Mahalanobis Distance to the statistical model is

$$\mathbf{b} = \mathbf{D}\mathbf{U}_x^T(\mathbf{U}_x\mathbf{D}\mathbf{U}_x^T)^{-1} . \tag{5}$$

The diagonal matrix $\mathbf{D}$ contains the eigenvalues. Plugging this into Eq.3 predicts the complete deformation.

2.3. Surrogate Signal Extraction

In order to drive the motion model, a surrogate signal of pulmonary motion is needed. Since we aim at motion compensation based on intra-operative X-ray images, the well visible change of diaphragm position is used as a surrogate signal with the individual steps explained as follows.

2.3.1. *DRR Generation.*

After registering the CT system with the X-ray, virtual DDR images can be determined from the CT volume using the same projection angle as the X-ray.

2.3.2. *Contour Generation.*

In the lung surface model that has been adapted to the pre-operative CT, the triangles close to the diaphragm are labelled. Based on a given projection angle, all labelled triangles are projected where $|\mathbf{n}_t \cdot \mathbf{n}_p^T| < 0.25$, with $\mathbf{n}_t$ the normal of the labelled triangle t and $\mathbf{n}_p$ the normal of the projection plane. Afterwards a spline is fitted through these points. As this is done separately for left and right lung, two contours are obtained.

2.3.3. *Contour Adaptation.*

By using an active contour approach, the left and right diaphragm contours can be easily adapted to a given X-ray image. In order to account for slight deviations during the contour generation process, the contours are re-adapted in the virtual projection. From the adapted contours, the surrogate signal can be extracted. Figure 2 shows the contour generation as well as the adapted contours in max-inhale and max-exhale virtual DRR images.

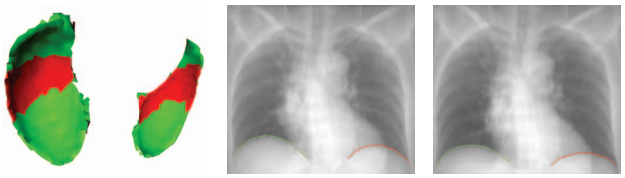


Fig. 2. Example of contour generation and adaptation. Left image shows diaphragm surfaces of adapted model with selected triangles (red). Derived contours that were adapted in max-inhale and max-exhale DRR images shown at right.

2.3.4. *Motion Model Input.*

From the adapted contours, the average displacement in head-foot direction is determined in CT space for left and right lung seperately. For the triangles projected into the projection plane during contour generation, we use those average displacements as input for our motion model to determine the weight vector in Eq. 5.

3. RESULTS

One critical part in the proposed workflow is the evaluation of the prediction result. While the intra-operative X-ray clearly shows bony structures and the outer lung surfaces, inner parts of the lungs, like airways or vessel tree, are hardly visible. Thus, defining anatomical landmarks in the X-ray images to evaluate the accuracy of the motion compensation is difficult. For that purpose, evaluation was carried out using the 4D-CT images in a leave-one-out manner. The motion model is built from all patients besides the one under consideration. From that particular patient, the CT belonging to the end exhale phase was chosen to correspond to the pre-operative CT. DRR images can finally be generated from all other phases that replace the intra-operative X-ray. As the transformation between the individual phases is known from the 4D-CT, this set-up allows for a quantification of the complete three-dimensional motion field at each location inside the lungs. The DRR images were generated to show a coronal view as those are mostly acquired in real procedures and the diaphragm change is most prominent from that perspective.

During the procedure, the X-ray is typically used as a 'snapshot' image to verify the location of the bronchoscope and device. Thus, it is typically not known to which phase of the breathing cycle the X-ray image belongs to. In order to overcome this problem, we reduced the proposed model that covers the whole breathing cycle to a simple two-phase model by only including the displacement from maximal exhale to maximal inhale. This means that we neglect any dynamic properties, as, e.g., hysteresis, and approximate breathing motion as a linear deformation over the breathing cycle. However, the reduced model is then able to adapt to X-ray images

of any arbitrary phase by 'scaling' the deformation according to the change in diaphragm.

For evaluation, we determine the error between maximum exhale and inhale as the difference between those phases is largest. The prediction result is evaluated by calculating the L_2-norm between predicted and estimated motion vectors in the inhale phase. The prediction results for all 31 cases are given in Fig. 3. In average, we were able to compensate for 56% of the motion amplitude with an average error of 4.06 ± 1.64 mm. In many cases, respiratory motion could be compensated significantly, e.g., ID 3. Furthermore, the error did not seem to be dependent on the average motion amplitude. However, there were also cases, especially ID 11 where compensation was quite difficult with a big remaining average error of more than 8 mm which was caused by the fact that the patient suffered from a severe pathology. The predicted motion fields were furthermore inspected for plausibility by calculating the Jacobian of the predicted motion field. The Jacobian allows to detect non-bijectively mapped regions (i.e., folding occurs). The evaluation showed that no folding occured for all cases. While the predictability of the complete three-dimensional motion field is of general interest, for this particular application the accuracy of the projected field is only important. The average error evaluated only in the projection reduces to 3.40 ± 1.58 mm, which means that 60% can be compensated.

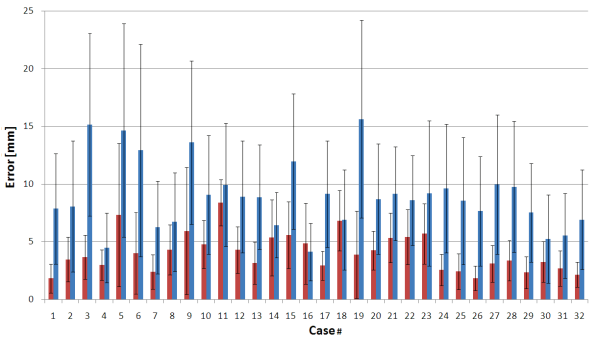


Fig. 3. Results of the motion prediction between maximal inhale and maximal exhale. Error after prediction (red) and motion amplitude (blue) are given in mm.

4. CONCLUSION

In contrast to previous contributions that focused on the model generation, we integrated in this work a general statistical motion model into a dedicated clinical scenario meaning CT/X-ray fusion during image-guided bronchoscopy. We accounted for application-specific conditions and investigated the ability to compensate for respiratory motion using a general model. As quantitative evaluation on real images is difficult, virtual projections were generated from 4D-CT data to simulate the intra-operative X-ray images belonging to different breathing states. Although the model was learned from different patients and the information derived from the projection images is limited, we were able to predict the lung motion between the phases of maximal distances with an average error of 4.06 ± 1.64 mm, which means that the model was able to compensate for 56% of the motion amplitude. Since the evaluation is based on opposite phase points, it can be expected that in a real application the residual error averaged over the breathing cycle is considerably smaller.

By working on 4D-CT, we were able to quantify the prediction error. However, in a real procedure, we expect additional complicating factors, e.g., deviations in the projection angle, registration error between CT and X-ray, but also questions like how is the breathing pattern affected by the bronchoscope. The evaluation carried out in this work gives a valuable estimate of the amount that can be compensated.

5. ACKNOWLEDGEMENTS

We would like to thank Paul Keall and Tokihiro Yamamoto for providing the image data from the Department of Radiation Oncology, Stanford University School of Medicine.

6. REFERENCES

[1] Q. Zhang and A. Pevsner et al., "A patient-specific respiratory model of anatomical motion for radiation treatment planning," *Med. Phys.*, vol. 34, no. 12, pp. 4772–4782, 2007.

[2] J. Ehrhardt and R. Werner et al., "Statistical modeling of 4D respiratory lung motion using diffeomorphic image registration," *IEEE Transactions on Medical Imaging*, vol. 30(2), pp. 251–265, 2011.

[3] T. He and Z. Xue et al., "Online 4D-CT estimation for patient-specific respiratory motion based on real-time breathing signals," in *Proc. of MICCAI*, 2010, vol. LNCS 6363, pp. 392–399.

[4] J. von Berg and H. Barschdorf et al., "Surface based cardiac and respiratory motion extraction motion extraction for pulmonary structures from multi-phase CT," in *Proc. of SPIE*, 2007, vol. 6511, pp. 65110Y1–11.

[5] S. Kabus and T. Klinder et al., "Evaluation of 4D-CT lung registration," in *Proc. of MICCAI*, 2009, vol. LNCS 5761, pp. 747–754.

[6] T. Blaffert and H. Barschdorf et al., "Lung lobe modeling and segmentation with individualized surface meshes," in *Proc. of SPIE Medical Imaging*, 2008., vol. 6914, pp. pp. 69141I1–10.